Effective radius of femtosecond laser radiation at its self-action in a gas medium in the multiple filamentation mode

A.A. Zemlyanov and A.D. Bulygin

V.E. Zuev Institute of Atmospheric Optics,
Siberian Branch of the Russian Academy of Sciences, Tomsk

Received September 11, 2008

Within the phenomenological approach with the use of multifocus model of filamentation, the equation for the Wigner function is derived to describe the propagation of high-power femtosecond laser pulse. In the approximation of the Gaussian profile of the mean intensity of laser radiation, the behavior of the laser beam effective radius is investigated.

Introduction

The propagation of high-power femtosecond laser pulses of terawatt and multiterawatt power[1,2] is accompanied by the self-action, giving rise to multiple filamentation. At a great number of filaments, multiple filamentation takes place in the so-called regime of optical turbulence,[3] which is a particular case of the strong turbulence. This regime is characterized by high-intensity structures of the optical field located in small spatial areas against a low-intensity background.[4]

The numerical investigation of the laser beam self-action in the multiple filamentation regime is described in Refs. 1 and 3.

Even with modern computers, it is quite problematic to study numerically the propagation of laser beams with fluctuating initial conditions and an initial radius of up to 100 mm to kilometer-long path lengths under conditions of the turbulent atmosphere.[5] In the cross sections of such beams, hundreds of filaments are formed.[2] Thus, it is important to develop a phenomenological method predicting the evolution of the main observed parameters of a laser beam, such as the energy, effective radius, and effective angular divergence, with the use of a finite number of parameters, determined from a numerical or laboratory experiment.

In Ref. 6 based on numerical calculations, the main stages of evolution of effective parameters in the regular regime of propagation of an axially symmetric laser beam were determined. In Ref. 7 based on the model of moving identical focuses,[8] the dependence of the effective radius on initial parameters and the light energy absorbed by the medium through the phenomenological parameter γ characterizing the transverse structure of a filament was established.

In this paper being a logical continuation of Ref. 7, the stochastic nonlinear Schrödinger equation (SNSE) is used in the multifocus model of filamentation to derive the equation for the Wigner function. This equation describes the propagation of a high-power laser pulse of a femtosecond duration in the regime of optical turbulence, characterized by the Bespalov–Talanov transverse instability and used in derivation of equations for effective parameters.

In solution of the derived nonclosed equations for effective parameters of a laser beam, it was proposed to introduce a phenomenological parameter $I_{\rm cr}$. This parameter characterizes the macroscopic intensity, at which the regime of optical turbulence takes place. To close the obtained system of equations for effective parameters of a laser beam, the macroscopic intensity of a laser beam was approximated by the Gaussian profile. The resultant relationships for averaged values of effective parameters and the corresponding averaged distribution of filaments agree with the commonly used estimates of the number of filaments.[1,3]

Equation for the Wigner function

The stochastic nonlinear Schrödinger equation has the following form:

$$\left\{\frac{\partial}{\partial z}-\frac{i}{2n_0k_0}\nabla_\perp^2+i\frac{k''_\omega\partial^2}{\partial t^2}\right\}\tilde U(\mathbf{r},t,z)-$$

$$-i\frac{k_0}{2}\left(\varepsilon_{NL}(\tilde I)+\tilde\varepsilon(\mathbf{r},z)\right)\tilde U(\mathbf{r},t,z)+\frac{\alpha_{NL}(\tilde I)}{2}\tilde U(\mathbf{r},t,z)=0 \quad (1)$$

with the random initial condition

$$\tilde U(\mathbf{r},t,z)\Big|_{z=0}=\tilde U_0(\mathbf{r},t).$$

Here k_0 is the wave number at the central frequency of radiation ω_0; n_0 is the refractive index of air;

0235-6880/08/12 928-06 $02.00 © 2008 Institute of Atmospheric Optics

$k''_\omega = \partial^2 k / \gamma\omega^2 |_{\omega=0}$ is the coefficient of the expansion of the wave number

$$k \approx k_0 + v_g^{-1}(\omega - \omega_0)^2 + k''_\omega(\omega - \omega_0)^2/2.$$

In Eq. (1), the nonlinear permittivity is represented as a sum

$$\varepsilon_{NL}(I) = \varepsilon_{\mathrm{ker}}(I) + \varepsilon_{\mathrm{pl}},$$

where

$$\varepsilon_{\mathrm{ker}}(I) = \varepsilon_{\mathrm{k}} I,\quad \varepsilon_{\mathrm{pl}}(I) = \eta_{\mathrm{cas}}\rho_{\mathrm{e}}(t)/2;$$

$\tilde{\varepsilon}$ is the fluctuating part of the permittivity in the atmosphere; $\alpha_{NL}(I)$ is the coefficient of nonlinear absorption of the medium (linear losses are neglected); η_{cas} is the rate of cascade ionization of a gas; $\rho_{\mathrm{e}}(t)$ is the concentration of free electrons determined from the evolution equation[5–7]; $\varepsilon_{\mathrm{ker}}(I)$ is the Kerr nonlinearity of the cubic type[9]; $\varepsilon_{\mathrm{pl}}$ is the permittivity of plasma; ε_{k} is the coefficient of the nonlinear addition to n_0.

Let us consider the spatiotemporal coherence function — the second-order moment

$$\Gamma(z,\bar{t},\mathbf{R},\tau,\boldsymbol{\rho}) = \langle \tilde{\psi}(z,\bar{t},\tau,\boldsymbol{\rho},\mathbf{R})\rangle_{\tilde{\varepsilon},\tilde{U}_0};$$
$$\tilde{\psi} \equiv \tilde{U}(z,\bar{t}-\tau/2,\mathbf{R}-\boldsymbol{\rho}/2)\tilde{U}^*(z,\bar{t}+\tau/2,\mathbf{R}+\boldsymbol{\rho}/2), \tag{2}$$

where

$$\mathbf{R} = (\mathbf{r}+\mathbf{r}')/2;\quad \boldsymbol{\rho} = (\mathbf{r}-\mathbf{r}')/2;$$
$$\bar{t} = (t+t')/2;\quad \tau = (t-t')/2;$$

(r, t) and (r', t') are two arbitrary points in space and time.

Differentiating Eq. (2) with respect to z and taking into account Eq. (1), we find

$$\frac{\partial}{\partial z}\Gamma(z,\bar{t},\mathbf{R},\tau,\boldsymbol{\rho}) = i\left(\frac{1}{n_0 k_0}\frac{\partial^2}{\partial\boldsymbol{\rho}\partial\mathbf{R}} - \frac{2k''_\omega\partial^2}{\partial\tau\partial\bar{t}}\right)\Gamma +$$
$$+ik_0\left\langle\left(\sinh\left(\frac{\boldsymbol{\rho}\partial}{2\partial\mathbf{R}}+\frac{\tau\partial}{2\partial\bar{t}}\right)\varepsilon_{NL}\left(\tilde{I}(z,\bar{t},\mathbf{R})\right)\right)\tilde{\psi}\right\rangle +$$
$$+ik_0\left\langle\left(\sinh\left(\frac{\boldsymbol{\rho}\partial}{2\partial\mathbf{R}}+\frac{\tau\partial}{2\partial\bar{t}}\right)\tilde{\varepsilon}(z,\bar{t},\mathbf{R})\right)\tilde{\psi}\right\rangle +$$
$$+\left\langle\left(\cosh\left(\frac{\boldsymbol{\rho}\partial}{2\partial\mathbf{R}}+\frac{\tau\partial}{2\partial\bar{t}}\right)\alpha_{NL}[\tilde{I}(z,\bar{t},\mathbf{R})]\right)\tilde{\psi}\right\rangle. \tag{3}$$

From the two-point field function $\tilde{\psi}$, we separate the regular part, namely, the coherence function Γ and the fluctuating part, namely, the function of a random perturbation $\delta\tilde{\psi}$:

$$\delta\tilde{\psi} \equiv \tilde{\psi} - \Gamma \to \tilde{I} = \langle\tilde{I}\rangle + \delta\tilde{I}.$$

Then equation (3) takes the following form:

$$\frac{\partial}{\partial z}\Gamma(z,\bar{t},\mathbf{R},\tau,\boldsymbol{\rho}) = i\left(\frac{1}{n_0 k_0}\frac{\partial^2}{\partial\boldsymbol{\rho}\partial\mathbf{R}} - \frac{2k''_\omega\partial^2}{\partial\tau\partial\bar{t}}\right)\Gamma +$$
$$+ik_0\varepsilon_{\mathrm{k}}\left(\sinh\left(\frac{\boldsymbol{\rho}\partial}{2\partial\mathbf{R}}+\frac{\tau\partial}{2\partial\bar{t}}\right)\langle\tilde{I}\rangle\right)\Gamma +$$
$$+ik_0\varepsilon_{\mathrm{k}}\left\langle\left(\sinh\left(\frac{\boldsymbol{\rho}\partial}{2\partial\mathbf{R}}+\frac{\tau\partial}{2\partial\bar{t}}\right)\delta\tilde{I}\right)\delta\tilde{\psi}\right\rangle +$$
$$+ik_0\left\langle\left(\sinh\left(\frac{\boldsymbol{\rho}\partial}{2\partial\mathbf{R}}+\frac{\tau\partial}{2\partial\bar{t}}\right)\tilde{\varepsilon}\right)\delta\tilde{\psi}\right\rangle +$$
$$+ik_0\left\langle\left(\sinh\left(\frac{\boldsymbol{\rho}\partial}{2\partial\mathbf{R}}+\frac{\tau\partial}{2\partial\bar{t}}\right)\varepsilon_{\mathrm{pl}}(\tilde{I})\right)\tilde{\psi}\right\rangle +$$
$$+\left\langle\left(\cosh\left(\frac{\boldsymbol{\rho}\partial}{2\partial\mathbf{R}}+\frac{\tau\partial}{2\partial\bar{t}}\right)\alpha_{NL}(\tilde{I})\right)\tilde{\psi}\right\rangle. \tag{4}$$

Using the procedure of the Fourier transform denoted hereinafter as $\hat{F}$, we pass to the spectral density of the Wigner function (brightness function) defined as follows:

$$J_\omega[z,\mathbf{R},\bar{t},\mathbf{n},\omega,k(\omega)] = \frac{c\sqrt{\varepsilon_0}}{8\pi}\hat{F}(\Gamma) \equiv$$
$$\equiv \frac{c\sqrt{\varepsilon_0}}{8\pi}(2\pi)^{-3}\int_{-\infty}^{\infty}\mathrm{d}\tau e^{-i\omega\tau}\int_{-\infty}^{\infty}\mathrm{d}\boldsymbol{\rho} e^{-k\mathbf{n}\boldsymbol{\rho}}\Gamma(z,\bar{t},\mathbf{R},\tau,\boldsymbol{\rho}), \tag{5}$$

where ε_0 is the permittivity of air; $\mathbf{n}$ is a unit vector.

Let $I \equiv \langle\tilde{I}\rangle$ have a rather smooth spatiotemporal profile, then we can neglect higher derivatives with respect to $\mathbf{R}$ and $\bar{t}$ in Eq. (4). From here, we have

$$\left[\frac{\partial}{\partial z} + \left(\frac{k}{n_0 k_0}\mathbf{n}\frac{\partial}{\partial\mathbf{R}} + \omega\frac{2k''_\omega\partial}{\partial\bar{t}}\right) + \frac{k_0\varepsilon_{\mathrm{k}}}{2k}\frac{\partial I}{\partial\mathbf{R}}\frac{\partial}{\partial\mathbf{n}} + \frac{k_0\varepsilon_{\mathrm{k}}}{2}\frac{\partial I}{\partial\bar{t}}\frac{\partial}{\partial\omega}\right]J_\omega =$$
$$= \frac{c\sqrt{\varepsilon_0}}{8\pi}\hat{F}\left[ik_0\varepsilon_{\mathrm{ker}}\left\langle\left(\sinh\left(\frac{\boldsymbol{\rho}\partial}{2\partial\mathbf{R}}+\frac{\tau\partial}{2\partial\bar{t}}\right)\delta\tilde{I}\right)\delta\tilde{\psi}\right\rangle +\right.$$
$$+ik_0\left\langle\left(\sinh\left(\frac{\boldsymbol{\rho}\partial}{2\partial\mathbf{R}}+\frac{\tau\partial}{2\partial\bar{t}}\right)\tilde{\varepsilon}\right)\delta\tilde{\psi}\right\rangle +$$
$$+ik_0\left\langle\left(\sinh\left(\frac{\boldsymbol{\rho}\partial}{2\partial\mathbf{R}}+\frac{\tau\partial}{2\partial\bar{t}}\right)\varepsilon_{pl}(\tilde{I})\right)\tilde{\psi}\right\rangle +$$
$$\left.+\left\langle\left(\cosh\left(\frac{\boldsymbol{\rho}\partial}{2\partial\mathbf{R}}+\frac{\tau\partial}{2\partial\bar{t}}\right)\alpha_{NL}(\tilde{I})\right)\tilde{\psi}\right\rangle\right]. \tag{6}$$

Then we pass from J_ω to the Wigner function $J = \int_{-\infty}^{\infty} J_\omega \mathrm{d}\omega$ and, neglecting the variance, obtain the equation for J

$$\left[\frac{\partial}{\partial z} + \frac{1}{n_0}\mathbf{n}\frac{\partial}{\partial\mathbf{R}} + \frac{1}{2}\frac{\partial}{\partial\mathbf{R}}\varepsilon_{\mathrm{ker}}(I)\frac{\partial}{\partial\mathbf{n}}\right]J = D + U + F. \tag{7}$$

Here, the following designations are introduced:

$$D \equiv \frac{c\sqrt{\varepsilon_0}}{8\pi}\int_{-\infty}^{\infty}\hat{F}\left[ik_0\left\langle\left(\sinh\left(\frac{\rho\partial}{2\partial\mathbf{R}}+\frac{\tau\partial}{2\partial\bar{t}}\right)\tilde{\varepsilon}\right)\delta\tilde{\psi}\right\rangle\right]d\omega; \quad (8a)$$

$$U \equiv \frac{c\sqrt{\varepsilon_0}}{8\pi}\int_{-\infty}^{\infty}\hat{F}\left(ik_0\varepsilon_{\text{ker}}\left\langle\left[\sinh\left(\frac{\rho\partial}{2\partial\mathbf{R}}+\frac{\tau\partial}{2\partial\bar{t}}\right)\delta\tilde{I}\right]\delta\tilde{\psi}\right\rangle\right)d\omega; \quad (8b)$$

$$F \equiv \frac{c\sqrt{\varepsilon_0}}{8\pi}\int_{-\infty}^{\infty}\hat{F}\left(ik_0\left\langle\left[\sinh\left(\frac{\rho\partial}{2\partial\mathbf{R}}+\frac{\tau\partial}{2\partial\bar{t}}\right)\varepsilon_{\text{pl}}(\tilde{I})\right]\tilde{\psi}\right\rangle + \left\langle\left[\cosh\left(\frac{\rho\partial}{2\partial\mathbf{R}}+\frac{\tau\partial}{2\partial\bar{t}}\right)\alpha_{NL}(\tilde{I})\right]\tilde{\psi}\right\rangle\right)d\omega. \quad (8c)$$

The function D determines the diffusion blooming of a laser beam. The function U is connected with field moments of the fourth order and, in particular, characterizes intensity fluctuations leading to the modulation instability of a laser beam and providing for the self-focusing of inhomogeneities of a certain size. Finally, the function F is expressed through nonlinear terms, whose contribution is significant only in the region of local focuses (filaments), and determines the absorption in a local focus, as well as its diffraction and defocusing properties.

For the further consideration, we accept *the approximation of local focuses with identical properties.* In this case, the function F can be represented in the following form:

$$F(z,\mathbf{R},\mathbf{n},\bar{t}) \approx \left\langle\tilde{N}(z,\mathbf{R},\bar{t})\right\rangle f(\mathbf{n}). \quad (9)$$

The function $f(\mathbf{n})$ can be found from either numerical or laboratory experiment. It characterizes the scattering and absorbing properties of a local focus. It can be determined through functions ε_{pl} and α_{NL} in the region of the maximal intensity of the light field. The parameters $\left\langle\tilde{N}(z,\mathbf{R},\bar{t})\right\rangle$ are the average concentrations of local focuses at each point of space and time.

Evolution of effective parameters

Below we will consider the following effective parameters[6]:

the energy transfer coefficient

$$T_{\text{e}}(z) = \int_{-\infty}^{\infty}I(z,\mathbf{R},\bar{t})d\mathbf{R}d\bar{t}\,/\,E(0), \quad (10a)$$

where

$$E(0) \equiv \int_{-\infty}^{\infty}I(0,\mathbf{R},\bar{t})d\mathbf{R}d\bar{t};$$

the effective radius and angular divergence of a laser beam

$$R_{\text{ef}}^2(z) \equiv \hat{R}_{\text{e}}^2(z)/T_{\text{e}}(z); \quad \theta_{\text{e}}^2(z) \equiv \hat{\theta}_{\text{e}}^2(z)/T_{\text{e}}(z), \quad (10b)$$

where

$$\hat{R}_{\text{e}}^2(z) = \int_{-\infty}^{\infty}I(z,\mathbf{R},\bar{t})\mathbf{R}^2d\mathbf{R}d\bar{t}\,/\,E(0);$$

$$\hat{\theta}_{\text{e}}^2(z) = \int_{-\infty}^{\infty}J(z,\mathbf{n},\mathbf{R},\bar{t})n^2d\mathbf{n}d\bar{t}d\mathbf{R}\,/\,E(0). \quad (10c)$$

From Eq. (7) taking into account Eqs. (8) and (9), we obtain the following equations for effective parameters:

$$\frac{\partial}{\partial z}T_{\text{e}}(z) = -\chi\int_{-\infty}^{\infty}\left\langle\tilde{N}\right\rangle d\mathbf{R}d\bar{t}, \quad \chi \equiv \chi_0/E(0), \quad (11)$$

$$\frac{\partial}{\partial z}\hat{R}_{\text{e}}^2 = 2\int_{-\infty}^{\infty}\mathbf{SR}d\mathbf{R}d\bar{t}\,/\,E(0) - \chi\int_{-\infty}^{\infty}\left\langle\tilde{N}\right\rangle\mathbf{R}^2d\mathbf{R}d\bar{t}. \quad (12)$$

Here

$$\mathbf{S} \equiv \int_{-\infty}^{\infty}J(z,\mathbf{n},\mathbf{R},\bar{t})\mathbf{n}d\mathbf{n}$$

is the transverse component of the Pointing vector; $\chi_0 \equiv -\int_{-\infty}^{\infty}f(\mathbf{n})d\mathbf{n}$ is the coefficient characterizing energy losses by a laser pulse due to absorption at one local focus. The last term in Eq. (12) is neglected below, because it is small.

Differentiating Eq. (12) again, we find

$$\frac{\partial^2}{\partial z^2}\hat{R}_{\text{e}}^2 = H + H_U + H_D + \mu\int_{-\infty}^{\infty}\left\langle\tilde{N}\right\rangle\mathbf{R}d\mathbf{R}d\bar{t}, \quad \mu \equiv \int\mathbf{n}f(\mathbf{n})d\mathbf{n}\,/\,E(0), \quad (13)$$

where

$$H = 2(\hat{\theta}_{\text{e}}^2 - \hat{\theta}_{\text{ker}}^2); \quad \hat{\theta}_{\text{ker}}^2 = \int_{-\infty}^{\infty}\varepsilon_{\text{ker}}(I)Id\mathbf{R}d\bar{t}\,/\,E(0), \quad (14a)$$

$$H_U = -\varepsilon_{\text{k}}\int_{-\infty}^{\infty}\left\langle\delta\tilde{I}\delta\tilde{I}\right\rangle d\mathbf{R}d\bar{t}\,/\,E(0), \quad H_D = \frac{c\sqrt{\varepsilon_0}}{8\pi}\int_{-\infty}^{\infty}\left\langle\delta\tilde{I}\frac{\partial}{\partial\mathbf{R}}\delta\tilde{\varepsilon}\right\rangle\mathbf{R}d\mathbf{R}d\bar{t}\,/\,E(0). \quad (14b)$$

The function H_U, characterizing the integral influence of intensity fluctuation of the light field, reaches the maximum in the region of multiple filamentation, where it is estimated as follows:

$$H_U \approx -(V_f / c)(\varepsilon_k I_f)^3 I_f \Big/ \int_{-\infty}^{\infty} \langle N \rangle \mathrm{d}\mathbf{R}\mathrm{d}\bar{t} \,/\, E(0),$$

where I_f is the intensity at a local focus; V_f is the volume of a local focus much smaller than the volume of a laser pulse, which is expressed by the following relationship:

$$V_f / t_\mathrm{p} c R_\mathrm{ef}^2 \ll 1; \; I_f \approx 5\cdot 10^{13}\,\mathrm{W/cm^2}; \; \varepsilon_k I_f \approx 1.5\cdot 10^{-5}.$$

From here, we can easily obtain the estimate $|H_U / H(0)| \ll 1$, which allows us to neglect H_U in Eq. (13).

The parameter H_D corresponds to the diffusion blooming of a laser beam. Let the length of the diffusion blooming be much shorter than the length of manifestation of nonlinear effects for a high-power laser pulse of the femtosecond duration, which allows us to neglect the term H_D. For the considered case of axial symmetry, the last term in Eq. (13) is zero. Differentiating Eq. (14a), we find

$$\frac{\partial}{\partial z}\hat{\theta}_\mathrm{e}^2 = \int \mathbf{S}\nabla_\perp \varepsilon_\mathrm{ker}(I)\mathrm{d}\mathbf{R}\mathrm{d}\bar{t} \,/\, E(0) + \gamma' \int_{-\infty}^{\infty} \langle \tilde{N} \rangle d\mathbf{R}\mathrm{d}\bar{t} +$$

$$+\varepsilon_k \int \langle \nabla_\perp \delta \mathbf{S} \delta \tilde{I} \rangle \mathrm{d}\mathbf{R}\mathrm{d}\bar{t} \,/\, E(0) + \frac{c\sqrt{\varepsilon_0}}{8\pi} \int \langle \nabla_\perp \delta \mathbf{S} \delta \tilde{\varepsilon} \rangle d\mathbf{R}\mathrm{d}\bar{t} \,/\, E(0), \tag{15a}$$

$$\frac{\partial}{\partial z}\hat{\theta}_\mathrm{ker}^2 = \int \mathbf{S}\nabla_\perp \varepsilon_\mathrm{ker}(I)\mathrm{d}\mathbf{R}\mathrm{d}\bar{t} \,/\, E(0) - \chi \varepsilon_\mathrm{ker} \int_{-\infty}^{\infty} I \langle \tilde{N} \rangle \mathrm{d}\mathbf{R}\mathrm{d}\bar{t}. \tag{15б}$$

Here $\gamma' \equiv \int f(\mathbf{n})\mathbf{n}^2 \mathrm{d}\mathbf{n} / E(0)$ characterizes the rate of increment of the squared angular divergence of a laser beam along the longitudinal coordinate after propagation of one local focus, which is determined both by diffraction effects upon energy absorption in a local focus and by defocusing properties in the formed plasma. The last term in Eq. (15a), responsible for the diffusion blooming, will be neglected by the above reasons. The third term in the right-hand side of Eq. (15a) can be estimated as $\chi \varepsilon_k I_f \int \langle N \rangle \mathrm{d}\mathbf{R}\mathrm{d}\bar{t}$. If we take it into account, the parameter γ' becomes slightly re-determined, and this change can be ignored.

The further analysis is possible with some additional assumptions, for example, *the hypothesis of critical intensity: we assume that as the macroscopic intensity achieves some threshold value* I_cr, *the state of maximal transverse instability takes place, at which the mean number of focuses* δN *in the laser beam cross section per unit area* δS *(focus density) with the intensity* $I \geq I_\mathrm{cr}$ *is determined as*

$$\delta N / \delta S = (P_{\delta S} / P_\mathrm{cr}) / \delta S = I / P_\mathrm{cr},$$

where $P_\mathrm{cr} \approx 3.2\cdot 10^9$ W is the critical power of the self-focusing in air.[9]

It is quite natural that isolated filaments are generated accidentally even before the laser pulse reaches the maximal intensity. However, we neglect the influence of these events on the evolution of effective parameters of a laser pulse. Starting only from the distance, at which the laser radiation intensity achieves the critical value, we believe that the mass filament generation takes place, and this point of the path is considered as a beginning of filamentation. For the qualitative analysis, we assume that the condition of the macroscopic (large-scale) Gaussiness is fulfilled, namely, the macroscopic intensity (averaged over spatial scales, which are much greater than the size of filaments) of a laser beam in the process of its propagation keeps the Gaussian profile with a constant duration t_p:

$$I(\mathbf{r},t,z) = I_0(z)\exp(-\mathbf{r}^2 / R_\mathrm{ef}^2 - t^2 / t_\mathrm{p}^2).$$

Within the framework of these assumptions in the zone of multiple filamentation $I_0(z) \geq I_\mathrm{cr}$ from Eqs. (11)–(15), we obtain a system of three ordinary differential equations for T_e, $\hat{\theta}_\mathrm{e}^2$ and $Y_\mathrm{e}^2 \equiv \hat{R}_\mathrm{e}^2(z)/\hat{R}_\mathrm{e}^2(z_{mf})$:

$$\begin{cases} \dfrac{\partial^2}{\partial z_R^2} Y_\mathrm{e}^2 = 2(\hat{\theta}_\mathrm{e}^2 - \hat{\theta}_\mathrm{ker}^2) L_R^2 / \hat{R}_\mathrm{e}^2(z_{mf}), \\ \dfrac{\partial}{\partial z_R}\hat{\theta}_\mathrm{e}^2 = \dfrac{\partial}{\partial z_R}\left[\hat{\theta}_\mathrm{ker}^2 + \gamma(1 - T_\mathrm{e})\right], \\ \dfrac{\partial}{\partial z_R} T_\mathrm{e}(z) = -L_R \chi N(T_\mathrm{e}, Y_\mathrm{e}^2); \end{cases} \tag{16}$$

$$N(T_\mathrm{e}, Y_\mathrm{e}^2) \equiv \int_{-\infty}^{\infty} \langle N(z,\bar{t},\mathbf{R}) \rangle \mathrm{d}\bar{t}\mathrm{d}\mathbf{R} = T_\mathrm{e}\left\{ \frac{I_\mathrm{cr}\hat{R}_\mathrm{e}^2(z_{mf})Y_\mathrm{e}^2}{\eta P_\mathrm{cr} T_\mathrm{e}^2} \times \right.$$

$$\left. \times \sqrt{\ln\left(\frac{\eta P_\mathrm{cr} T_\mathrm{e}^2}{I_\mathrm{cr}\hat{R}_\mathrm{e}^2(z_{mf})Y_\mathrm{e}^2}\right)} - \mathrm{erf}\left[\sqrt{\ln\left(\frac{\eta P_\mathrm{cr} T_\mathrm{e}^2}{I_\mathrm{cr}\hat{R}_\mathrm{e}^2(z_{mf})Y_\mathrm{e}^2}\right)}\right]\right\},$$

where

$$L_R = k_0 \hat{R}_0^2 / 2; \; z_R = z / L_R; \; \gamma = \gamma_0 + \sqrt{8}\varepsilon_k I_\mathrm{cr}; \; \eta = P_0 / P_\mathrm{cr};$$

z_{mf} is the coordinate of the beginning of filamentation; the parameter $\gamma_0 \equiv \gamma' / \chi$ is found in Ref. 7 ($\gamma_0 \approx 1.3\cdot 10^{-5}$); P_0 and R_0 are the average values of the power and radius of a laser beam, respectively.

The initial conditions for the system (16) at the entrance into the filamentation zone such as $V_{mf} \equiv \partial \hat{R}_\mathrm{e}^2 / \partial z$, z_{mf} and $R_\mathrm{e}^2(z_{mf})$, are determined from the following equations[9]:

$$\hat{R}_\mathrm{e}^2(z_{mf}) = \hat{R}_0^2\left[\left(1 - \frac{\eta}{b}\right)\left(\frac{z_{mf}}{2L_R}\right)^2 + \left(1 + \frac{V_0 z_{mf}}{2}\right)^2\right], \; b = 1.62;$$

$$H_0 = (1-\eta/b)\frac{2}{\hat{R}_0^{2} k_0^{2}} + \frac{1}{2}\hat{R}_0^{2}\hat{V}_0^{2}, \quad V_0 \equiv \partial \hat{R}_e^{2} / \partial z\big|_{z=0}. \quad (17)$$

Here H_0 is the so-called Hamilton function of a laser beam in a Kerr medium[9]; V_0 corresponds to the initial curvature of the phase front.

In the approximation of the Gaussian profile of the laser pulse intensity, we find the filamentation point z_{mf} from the condition that the maximal intensity of a laser beam $I(z)$ achieves the critical value I_{cr}:

$$I(z_{mf}) = E(0)^2 / \hat{R}_e^{2}(z_{mf}) = I_{cr}, \quad (18a)$$

then

$$V_{mf} = V_0 + H_0 z_{mf}. \quad (18b)$$

The solution of Eq. (16) with the initial conditions, determined from Eqs. (17) and (18), can be easily found numerically. The model parameters $I_{cr} \approx 2.5\cdot 10^{12}$ W/cm^2 and $\chi \approx 0.64\cdot 10^{-4}$ J were determined from the comparison with results of numerical calculation for a laser beam with the radius $R_0 = 2$ mm and the initial power $\eta \equiv P_0 / P_{cr} = 88$ in the regime of multiple filamentation[1] at the beginning and at the end of multiple filamentation (Fig. 1).

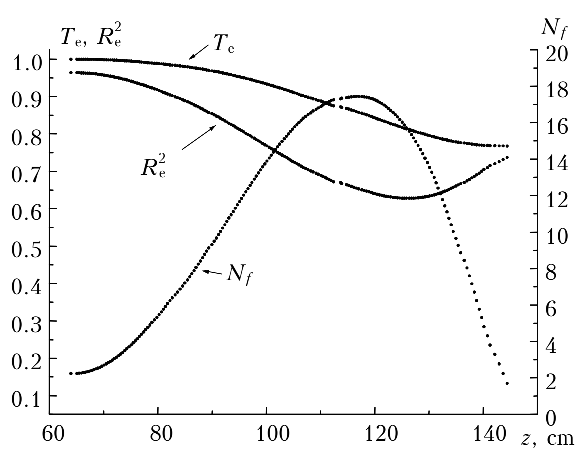

Fig. 1 Energy transfer coefficient T_e, normalized initial value of the squared effective radius R_e^2, and the number of filaments N_f along the propagation path at $R_0 = 2$ mm and $P_0 = 88P_{cr}$.

If we determine the average number of filaments N_f through the density of focuses in the central temporal cross section of a laser pulse: $N_f(z) \equiv \int_{-\infty}^{\infty} N(\mathbf{R},0,z)\mathrm{d}\mathbf{R}$, then in the Gauss approximation we find $N_f = \eta(T_e - Y_e^2/T)$. As can be seen from Figs. 1 and 2, the obtained distribution of filaments along the propagation path agrees with the used estimate of the number of filaments $N_f \approx P_0/P_f$, where $P_f \approx (3–5)P_{cr}$ [Ref. 1]. This fact indicates the adequacy of the proposed model of multiple filamentation.

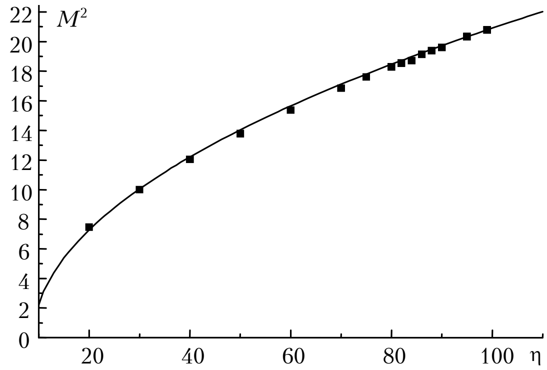

Fig. 2. Propagation coefficient after passage of the global focus as a function of $\eta = P_0/P_{cr}$ for the regime of multiple filamentation at $R_0 = 2$ mm: results obtained by numerical solution of the system of Eq. (18) (squares) and Eq. (21) (solid curve).

Figure 2 shows the propagation coefficient M^2 [Refs. 6 and 7] after passage of the global focus as a function of the initial power. For comparison of the regimes of single and multiple filamentation, figure 3 shows the filamentation length L_f, function T_e, and waist radius R_w^2.

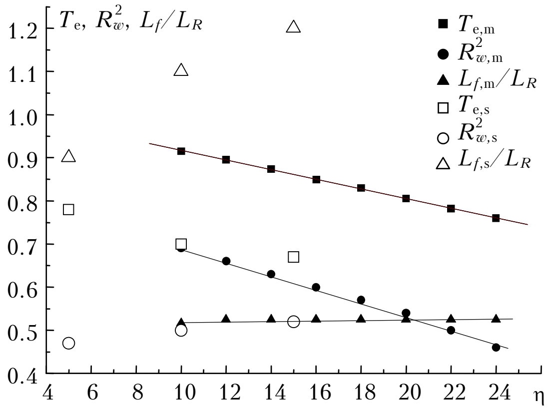

Fig. 3. Energy transfer coefficient T_e, effective value of the squared waist radius R_w^2 normalized to R_0^2, and filamentation length normalized to the Rayleigh length L_f/L_R as functions of $\eta = P_0/P_{cr}$ for the regimes of multiple filamentation (subscripted by m) (for illustration, the points obtained from numerical experiment are connected by straight lines) and single filamentation at $R_0 = 1$ mm (subscripted by s).

Figure 4 shows the propagation coefficient for the regimes of single M_s^2 and multiple M_m^2 filamentation calculated by the approximation equations (19):

$$M_s^2(\eta, R_0^2) = 2\sqrt{H_0/(L_R k_0) + C_s(R_0)\eta}, \quad (19a)$$

$$M_m^2(\eta, R_0^2) = 2\sqrt{H_0/(L_R k_0) + (C_m\eta - \beta R_0^2)}, \quad (19b)$$

where $C_s|_{R_0=1\text{ mm}} \approx 4$; $C_m \approx 9$; $\beta \approx 4$ mm^{-2} are the introduced empirical constants, characterizing the dependence of the increment of the squared angular divergence after the passage through the nonlinear layer on η. It should be noted that equation (19b) is true only under the condition $\eta C_m \gg \beta R_0^2$. This restriction is a consequence of the used approximation of the Gaussian profile of the laser beam intensity.

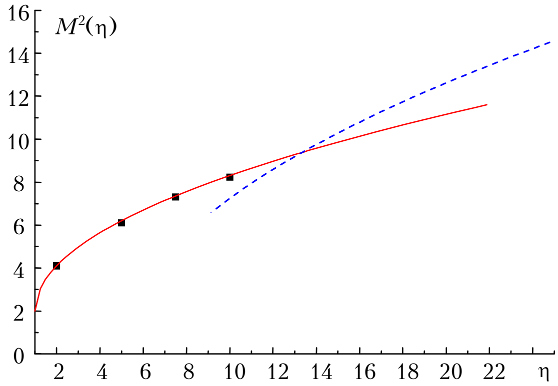

Fig. 4. Propagation coefficient after the passage of the point of global focus as a function of $\eta = P_0/P_{cr}$ for the regime of single (solid curve) and multiple (dash curve) filamentation at $R_0 = 1$ mm.

It follows from Fig. 3 that as $\eta = P_0 / P_{cr}$ increases, the waist radius decreases linearly with the distance, whereas the filamentation length increases, and the energy transfer coefficient decreases.

Conclusions

The equation for the Wigner function (7) is proposed based on SNSE within the phenomenological approach with the use of the multifocus filamentation model for the description of propagation of a high-power femtosecond laser pulse in the regime of the optical turbulence. The formulated equations for the Wigner function have been used to derive equations for effective parameters of a laser beam, studied using the hypothesis on the critical intensity for the regime of the optical turbulence in the approximation of the Gaussian intensity profile (16). The filament distribution, obtained from the numerical solution of Eqs. (18) and (19) along the propagation path, agrees with the commonly used estimate of the filament number as $N_f \approx P_0/P_f$, where $P_f \approx (3–5)P_{cr}$. This fact indicates the adequacy of the model and the used approximations. In particular, it confirms the hypothesis that the critical intensity achieving $2.5 \cdot 10^{12}$ W/cm^2 exists for the optical turbulence regime.

It has been found that regularities in the evolution of effective parameters in the regimes of multiple and single filamentation are qualitatively similar.[6] In particular, the squared propagation coefficient after passage of the global focus was found to depend linearly on the initial power of the laser pulse (19).

Acknowledgements

This work was supported in part by Combined Integration Project No. 3.13 and Russian Foundation for Basic Research (Grant No. 06-05-64799).

References

1. S. Skupin, L. Berge, U. Peschel, F. Lederer, G. Mejean, J. Yu, J. Kasparian, E. Salmon, J.P. Wolf, M. Rodriguez, L. Woste, R. Bourayou, and R. Sauerbrey, Phys. Rev. E **70**, 046602-1–046602-15 (2004).
2. P. Bejot, L. Bonacina, J. Extermann, M. Moret, J.P. Wolf, R. Ackermann, N. Lascoux, R. Salame, J. Kasparian, L. Berge, S. Champeaux, C. Guet, N. Blanchot, E. Mazataud, G. Mennerat, L. Patissou, V. Prevot, D. Raffestin, and J. Ribolzi, Appl. Phys. Lett. **90**, 151106-1–151106-3 (2007).
3. M. Mlejnek, M. Kolesik, J.V. Moloney, and E.M. Wright, Phys. Rev. Lett. **83,** 2938–2941 (1999).
4. P.A. Robinson, Rev. of Mod. Phys. **69**, No. 2, 507–573 (1997).
5. S.A. Shlyonov, V.Yu. Fedorov, and V.P. Kandidov, Atmos. Oceanic Opt. **20**, No. 4, 275–283 (2007).
6. A.A. Zemlyanov and Yu.E. Geints, Atmos. Oceanic Opt. **18**, No. 7, 514–519 (2005).
7. A.D. Bulygin, A.A. Zemlyanov, and Yu.E. Geints, Atmos. Oceanic Opt. **20**, No. 11, 887–893 (2007).
8. V.N. Lugovoi and A.M. Prokhorov, JETP. Lett. **7**, No. 5, 117–119 (1968).
9. S.N. Vlasov and V.I Talanov, *Self-Focusing of Waves* (Nizhny Novgorod, 1997), 220 pp.